Supplementary Material

Enhanced dark catalytic reduction of organic dyes and heavy-metal pollutants over activated carbon-supported V/S-BiOBr

Mengistu Tadesse Mosisa[a, c], Samuel Ndaghiya Adawara[a], Adugna Boke Abdeta[d], Benjamin Kunkadma Inusa[a], Cuizhu Li[a], Haoyv Wang[a], Kening Xiang[a], Dong-Hau Kuo[b], Jinguo Lin*[, a], Xiaoyun Chen*[, a]

[a] College of Materials Engineering, Fujian Agriculture and Forestry University, Fuzhou 350002, China

[b] Department of Materials Science and Engineering, National Taiwan University of Science and Technology, Taipei 106335, Taiwan

[c] Department of Chemical Engineering, Adama Science and Technology University, Adama, Ethiopia

[d] Department of Chemistry, Jimma University, Jimma, Ethiopia

*Corresponding author

E-mail address: fjlinjg@126.com (J. Lin)

E-mail address: fjchenxy@126.com (X. Chen)

CONTENTS

1 Additional figures

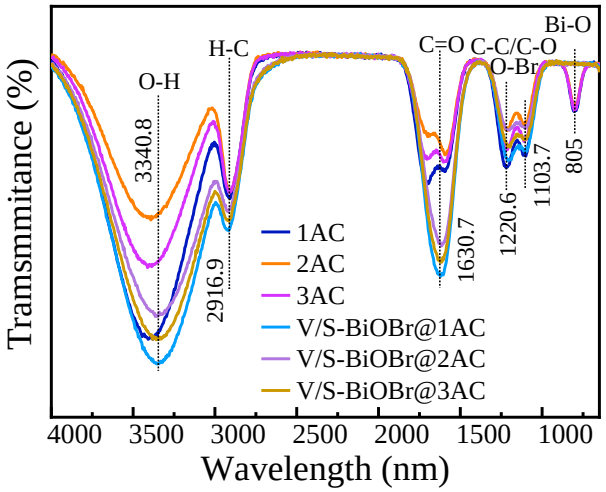

Fig.S1 FTIR spectra of 1AC, 2AC, 3AC, V/S-BiOBr@1AC, V/S-BiOBr@2AC, and V/S-BiOBr@3AC.

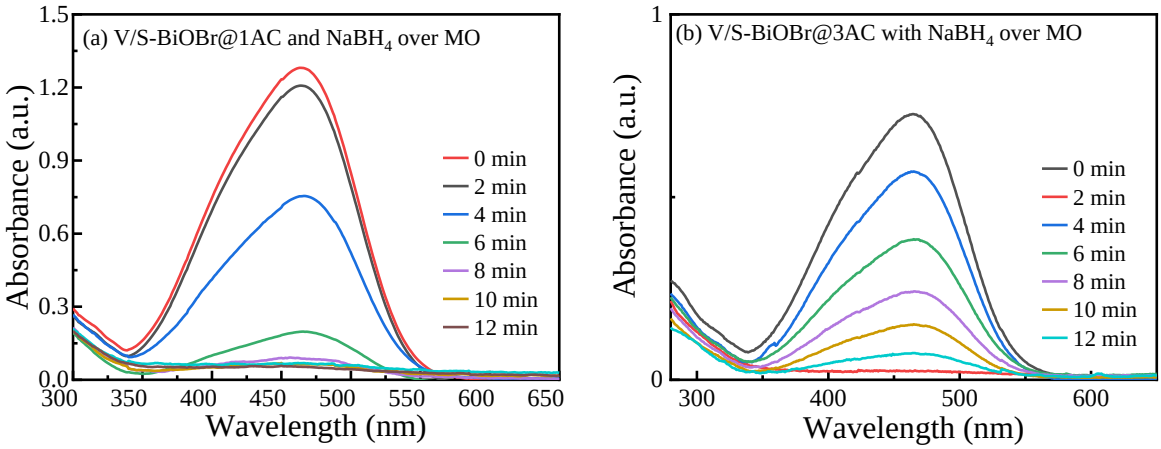

Fig. S2 Reduction of MO: (a) with V/S-BiOBr@1AC and $NaBH_4$, (b) with V/S-BiOBr@3AC and $NaBH_4$.

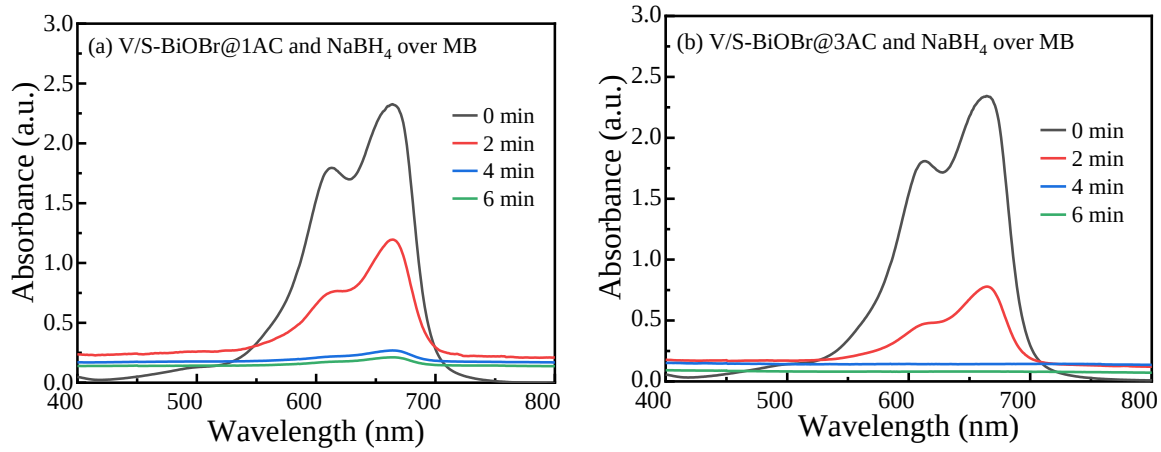

Fig. S3 Reduction of MB: (a) with V/S-BiOBr@1AC and $NaBH_4$, (b) with V/S-BiOBr@3AC and $NaBH_4$.

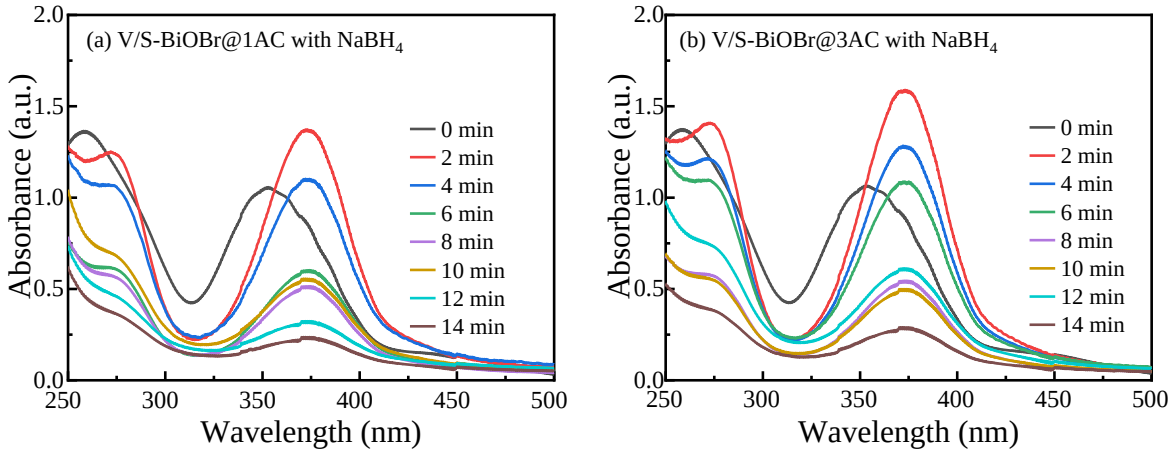

Fig. S4 Reduction of Cr(VI): (a) with V/S-BiOBr@1AC and $NaBH_4$, (b) with V/S-BiOBr@3AC and $NaBH_4$.

2 Additional tables

Table S1 XPS composition, oxygen vacancy (Vo) content, crystallite size, and S_{BET} of V/S-BiOBr and V/S-BiOBr@2AC

Catalyst	Atomic percentage (%)						$V^{4+}/(V^{4+}+V^{5+})$ (%)	V_O (%)	Crystal size (nm)	S_{BET} (m^2/g)	Pore volume (cm^3/g)
	V	Bi	O	Br	S	C					
V/S-BiOBr	8.7	34.6	22.6	17.3	14.1	2.7	36.6	5.3	17.8	14	0.148
V/S-BiOBr@2AC	8.6	34.4	13.3	16.9	14.2	13.6	32.3	15.5	25.7	42	1.08
V/S-BiOBr@2AC after used	8.5	34.2	13.1	16.3	14.6	13.3	31.3	19.6	25.6	42	1.07

Table S2 Element contents from SEM-EDS analysis for V/S-BiOBr and V/S-BiOBr@2AC

Catalyst	V	Bi	O	Br	S	C
V/S-BiOBr	8.6	34.3	22.4	17.2	14.7	2.8
V/S-BiOBr@2AC	8.7	34.2	13.3	16.3	14.2	13.3

Table S3 XRF chemical element compositions of V/S-BiOBr and V/S-BiOBr@2AC

Catalyst	V	Bi	O	Br	S	C
V/S-BiOBr	8.5	34.4	21.5	17.3	14.4	2.7
V/S-BiOBr@2AC	8.6	34.2	12.6	14.1	14.5	12.3

Table S4 Elemental composition of activated carbon

Activated carbon type	Status	C (%wt)	H (%wt)	N (%wt)	O (%wt)	Ash (% wt)
Micro porous	Fresh/commercial	85±2	0.41±0.5	0.52±0.07	1±2	13+0.09
Mesoporous	Fresh/commercial	84±2	0.47±0.06	0.54±0.08	1±2	12±0.08
Micro-mesoporous	Fresh/commercial	85±2	0.43±0.08	0.52±0.09	1±2	13±0.09

Table S5 Porosity and types of activated carbon used in the research

Types of Activated Carbon	Surface area (m^2/g)	Pore volume (cm^3/g)
Microporous activated carbon (1AC)	1479	1.05
Mesoporous activated carbon (2AC)	812	1.45
Micro-meso activated carbon (3AC)	1413	1.46

Table S6 Elemental composition and N_2 physisorption comparison of fresh and spent V/S-BiOBr@2AC

Sample	Wt %					Retention %					m^2/g	cm^3/g		
	V	S	Bi	O	Br	V	S	Bi	O	Br	S_{BET}	Pore in micro	Pore in meso	Total pore
Fresh V/S-BiOBr@2AC	2.1	1.8	38.5	8.4	17.6	-	-	-	-	-	420	0.18	0.42	0.60
Spent V/S-BiOBr@2AC	2.0	1.7	37.4	8.1	16.9	94	92	97	96	96	398	0.16	0.39	0.55

Table S7 Comparison of V/S-BiOBr@2AC reduction of MB, MO, and Cr(VI) with reported literature

Pollutants	Catalyst	Solution volume (mL)	$NaBH_4$ [mmol/L]	Catalyst dose (mg)	Time (min)	k_{app} (min^{-1})	K (min/g)	Ref.
MB	Ce-BiOBr/Bi_2S_3	100	0.04	5	14	0.231	23.1	[1]
	$Cu(MoO_4)_2(OH)_2$	1000	0.04	5	20	0.021	2	[2]
	Mn_3O_4/ZnO/AC)	100	0.01	10	20	0.03	3	[3]
	PANI@$NiTiO_3$	100	0.04	50	60	0.05	5	[4]
	MgO	100	0.04	40	60	0.02	2	[5]
	V/S-BiOBr@2AC	100	0.04	5	14	0.4383	43.83	This work
MO	V/S-SnO_2	100	0.04	20	6	0.211	21.1	[6]
	V/O-Ag_2S	100	0.04	20	10	0.289	28.9	[7]
	Fe/S-BiOCl	100	0.04	20	14	-	-	[8]
	Co/S-CeO_2	100	0.04	20	10	-	-	[9]
	S-$CoMoO_4.0.9H_2O$	100	0.04	10	6	-	-	[10]
	V/S-BiOBr@2AC	100	0.04	5	6	0.4284	42.84	This work
Cr(IV)	V/S-BiOBr	100	0.04	5	18	0.03	3	[11]
	Mn/O-Bi_2S_3	100	0.01	10	20	0.04	4	[12]
	Cu/Cu_2O/NH_2-MIL-88B(Fe)	100	0.05	50	20	0.05	5	[13]
	$CsPbBr_3$/CdS	100	0.01	50	30	0.07	7	[14]
	$Cu_3(MoO_4)_2(OH)_2$	100	0.04	10	60	1.09	109	[2]
	MoSrOS	100	0.04	5	14	0.171	17.1	[15]
	O-$Sn_{17}Sb_6S_{29}$	100	0.01	10	6	0.09	9	[16]
	La/O-SnS	100	0.01	5	18	0.364	36.4	[17]
	V/S-BiOBr@2AC	100	0.04	5	18	0.2178	21.78	This work

References:

[1] Mosisa M T, Zhang P, Wu B. Chen L, Su Z, Li P, Zhang H, Farooq A, Huang T, Abdeta AB, Zelekew OA, Kuo DH, Lin J, Chen X, Lu D. Synthesis and characterization of Ce-BiOBr/Bi_2S_3 catalyst with enhanced catalytic activity for organic dye reduction under dark, *J. Environ. Chem. Eng.*, 12 (2024) 113383.

[2] Q. Wu, P. Zhang, D.-H. Kuo, B. Wu, A.B. Abdeta, Z. Su, L. Chen, O.A. Zelekew, J. Lin, X. Chen, Activation of $Cu_3(MoO_4)_2(OH)_2$ with the hydrazine-driven cation reduction into a highly efficient catalyst for the reduction of organic dyes and heavy metals ion, *J. Environ. Chem. Eng.*, 11 (2023) 109974.

[3] Nguyen, H. T.; Doan, V.-D.; Nguyen, T. L. H.; Nguyen, A.-T.; Tran, Q.-H.; Tran, V. A.; Le, V. T, Mechanistic pathway and optimization of rhodamine B degradation using Mn_3O_4/ZnO nanocomposite on microalgae-based carbon, *RSC Adv*., 15 (2025) 6241-6259.

[4] Abouri, M.; Benzaouak, A.; Elouardi, M.; El Hamdaoui, L.; Zaaboul, F.; Azzaoui, K.; Hammouti, B.; Sabbahi, R.; Jodeh, S.; El Belghiti, M. A.; El Hamidi, A, Enhanced photocatalytic degradation of Rhodamine B using polyaniline-coated $XTiO_3$ (X = Co, Ni) nanocomposites, *Sci. Rep*., 15 (2025) 3595.

[5] Gatou, M.-A.; Bovali, N.; Lagopati, N.; Pavlatou, E. A, MgO nanoparticles as a promising photocatalyst towards rhodamine B and rhodamine 6G degradation, *Molecules*, 29 (2024) 4299.

[6] Yang, B.; Wu, X.; Su, Z.; Insua, B. K.; Zhang, P.; Kuo, D.-H.; Gao, L.; Bao, X.; Lu, D.; Lin, J.; Chen, X, Heterovalent state and oxygen vacancy defect structure-associated V/S co-doped SnO_2

for catalytic reduction of organic and Cr^{6+} pollutants in the dark, *Adv. Sustain*. Syst., 8 (2024) 2400429.

[7] Wu B, Su Z, Wu Q, Kuo DH, Zhang P, Chen L, Abdeta AB, Mosisa MT, Lin J, Chen X, Liu X. Mn/O co-doped Bi_2S_3 bimetal oxysulfide catalyst for highly efficient reduction of organic and hexavalent chromium pollutants in the dark, *Mater. Today Chem*., 33 (2023) 101697.

[8] Li, C.; Wang, H.; Liu, T.; Zhang, P.; Li, Q.; Xiang, K.; Kuo, D.-H.; Lu, D.; Mosisa, M. T.; Liao, Y.; Lin, J.; Chen, X, Fe/S co-doped BiOCl sulfur-oxychloride for efficient catalytic reduction of organic and Cr^{6+}: synergistic regulation of heterovalent states and oxygen vacancy defects, *J. Water Process Eng*., 75 (2025) 108093.

[9] Zhang, P.; Wang, H.; Lai, Y.; Xu, Y.; Chen, L.; Wu, Q.; Kuo, D.-H.; Lu, D.; Mosisa, M. T.; Li, J.; Lin, J.; Chen, X, Synergistic Co/S co-doped CeO_2 sulfur-oxide catalyst for efficient catalytic reduction of toxic organics and heavy metal pollutants under dark conditions, *J. Water Process Eng.*, 58 (2024) 104820.

[10] Zhang, P.; Wu, Q.; Wang, H.; Xu, Y.; Lai, Y.; Li, P.; Kuo, D.-H.; Huang, T.; Zhang, H.; Mosisa, M. T.; Li, J.; Lin, J.; Chen, X.; Lu, D, Hydrazine-driven cation valence regulation and oxygen defect engineering in sulfur-doped $CoMoO_4 \cdot 0.9H_2O$ for highly efficient reduction of toxic organics and hexavalent chromium under dark, *Mater. Today, Chem*., 37 (2024) 102028.

[11] Mosisa, M. T.; Zhang, P.; Su, Z.; Wu, B.; Chen, L.; Liao, Y.; Farooq, A.; Lu, D.; Abdeta, A. B.; Kuo, D.-H.; Lin, J.; Chen, X, A novel V/S co-doped BiOBr catalyst for high-efficiency catalytic reduction of toxic organic and hexavalent chromium pollutants under dark, *J. Environ.*

Chem. Eng.,12 (2024) 112111.

[12] Wu, B.; Su, Z.; Wu, Q.; Kuo, D.-H.; Zhang, P.; Chen, L.; Abdeta, A. B.; Mosisa, M. T.; Lin, J.; Chen, X.; Liu, X, Mn/O co-doped Bi_2S_3 bimetal oxysulfide catalyst for highly efficient reduction of organic and hexavalent chromium pollutants in the dark, *Mater. Today, Chem*., 33 (2023) 101697.

[13] Xu, C, $Cu/Cu_2O/NH_2$-MIL-88B(Fe) heterojunction as the photocatalyst to remove hexavalent chromium heavy metal ions in water, *RSC Adv*., 15 (2025) 2462-2469.

[14] Kipkorir, A.; DuBose, J.; Cho, J.; Kamat, P. V, $CsPbBr_3$-CdS heterostructure: stabilizing perovskite nanocrystals for photocatalysis, *Chem. Sci*., 12 (2021) 14815-14825.

[15] Wu, Q.; Wang, X.; Fu, J.; Zelekew, O. A.; Abdeta, A. B.; Kuo, D.-H.; Zhang, J.; Yuan, Z.; Lin, J.; Chen, X, Wool-coiled bimetallic oxysulfide MoSrOS catalyst synthesis for catalytic reduction of toxic organic pollutants and heavy metal ions, *J. Sci. Adv. Mater. Devices*, 6 (2021) 578-586.

[16] Huang, T.; Li, P.; Wu, Q.; Abdeta, A. B.; Kuo, D.-H.; Zhang, H.; Wu, B.; Mosisa, M. T.; Lin, J.; Chen, X.; Liu, X, Oxygen-doped $Sn_{17}Sb_6S_{29}$ bimetal oxysulfide catalysts for efficient reduction of organic pollutants and hexavalent chromium in the dark, *React. Chem. Eng*., 9 (2024) 410-425.

[17] Zhang, H.; Zhang, P.; Su, Z.; Kuo, D.-H.; Wu, Q.; Huang, T.; Li, P.; Mosisa, M. T.; Lin, J.; Chen, X.; Lu, D, Synergistic hydrogen peroxide-driven cation valence regulation and La/O co-doped SnS-based oxysulfide catalyst for efficient catalytic reduction of toxic organics and Cr (VI) under dark, *Adv. Sustain. Syst*., 8 (2024) 2400212.